Dalton
www.rsc.org/dalton

Luminescent cyclometallated rhodium(III) bis(pyridylbenzaldehyde) complexes with long-lived excited states

Kenneth Kam-Wing Lo,*[a] Chi-Kwan Li,[a] Kin-Wai Lau[a] and Nianyong Zhu[b]

[a] *Department of Biology and Chemistry, City University of Hong Kong, Tat Chee Avenue, Kowloon, Hong Kong, P. R. China. E-mail: bhkenlo@cityu.edu.hk; Fax: (+852) 2788 7406*

[b] *Department of Chemistry, The University of Hong Kong, Pokfulam Road, Hong Kong, P. R. China*

Received 8th September 2003, Accepted 7th October 2003
First published as an Advance Article on the web 14th October 2003

A series of luminescent cyclometallated rhodium(III) diimine complexes containing two aldehyde functional groups $[Rh(pba)_2(N–N)]Cl$ (Hpba = 4-(2-pyridyl)benzaldehyde; N–N = 2,2′-bipyridine, bpy (**2**); 4,4′-dimethyl-2,2′-bipyridine, 4,4′-Me_2bpy (**3**); 1,10-phenanthroline, phen (**4**); 3,4,7,8-tetramethyl-1,10-phenanthroline, 3,4,7,8-Me_4phen (**5**); 4,7-diphenyl-1,10-phenanthroline, 4,7-Ph_2phen (**6**)) have been synthesised, and their photophysical and electrochemical properties investigated. The X-ray crystal structures of complexes **3**, **4** and the precursor complex, $[Rh_2(pba)_4Cl_2]$ (**1**), have also been determined. Upon photoexcitation, complexes **2**–**6** display long-lived emission in solutions at 298 K and in low-temperature glass. Remarkably, the luminescence lifetimes of the complexes in solutions at 298 K are extraordinarily long (*ca.* 4.2–8.7 μs). To the best of our knowledge, there is no precedent for such long emission lifetimes observed in other related cyclometallated rhodium(III) systems. The solution emission spectra show structured bands with emission maxima at *ca.* 506 nm. The emission is tentatively assigned to an excited state of triplet intra-ligand ^{3}IL ($\pi \longrightarrow \pi^*$)(pba$^-$) character, probably mixed with some triplet metal-to-ligand charge-transfer ^{3}MLCT (d_π(Rh) $\longrightarrow \pi^*$(pba$^-$)) character. On the basis of the facile reaction between the aldehyde group and the primary amine group, to form a secondary amine after reductive amination, complexes **2**–**6** have been used to label the protein bovine serum albumin. The photophysical properties of the bioconjugates have also been investigated.

Introduction

The photophysical and photochemical studies of luminescent polypyridine complexes of d^6 transition metals such as ruthenium(II), osmium(II), rhenium(I), iridium(III) and rhodium(III) have attracted much attention since the emission and excited-state properties of these complexes can be readily tuned by altering the identities of the metal centre and ligands.[1] In particular, luminescent iridium(III) and rhodium(III) complexes have received increasing interest because of their high structural variation, and intriguing photophysical properties.[2–5]

On the other hand, the development of fluorescent tags for biological molecules has been well documented.[6,7] These labels offer a wide range of emission colours, and many choices of the reactive functional groups for bioconjugation are available. The use of fluorescent cross-linking reagents for biomolecules has also been investigated.[6–9] Recently, we reported a series of luminescent iridium(III) diimine complexes containing two aldehyde functional groups as biological labelling reagents.[10] The aldehyde moieties of these complexes allow them to react with the primary amine groups of biomolecules to give luminescent bioconjugates. The photophysical properties of the labelled biomolecules have been studied. In view of the interesting photophysical and photochemical properties of rhodium(III) diimine complexes,[2c–e,3b–d,4b–d,5] and the utilisation of these complexes in the photo-induced electron-transfer studies of nucleic acids,[11] we are interested in the possibility of using luminescent cyclometallated rhodium(III) diimine complexes as biological labelling reagents. In the current work, a series of luminescent cyclometallated rhodium(III) diimine complexes containing two aldehyde functional groups $[Rh(pba)_2(N–N)]Cl$ (Hpba = 4-(2-pyridyl)benzaldehyde; N–N = 2,2′-bipyridine, bpy (**2**); 4,4′-dimethyl-2,2′-bipyridine, 4,4′-Me_2bpy (**3**); 1,10-phenanthroline, phen (**4**); 3,4,7,8-tetramethyl-1,10-phenanthroline, 3,4,7,8-Me_4phen (**5**); 4,7-diphenyl-1,10-phenanthroline, 4,7-Ph_2phen (**6**)) and their dimeric precursor complex $[Rh_2(pba)_4Cl_2]$ (**1**) have been synthesised and characterised (Scheme 1). The X-ray crystal structures of complexes **1**, **3** and **4** have also been determined. The photophysical and electrochemical properties of these complexes have been studied. On the basis of the facile reaction between the aldehyde group and the primary amine group, to form a secondary amine after reductive amination, complexes **2**–**6** have been used to label the protein bovine serum albumin (BSA). The photophysical properties of the bioconjugates have also been investigated.

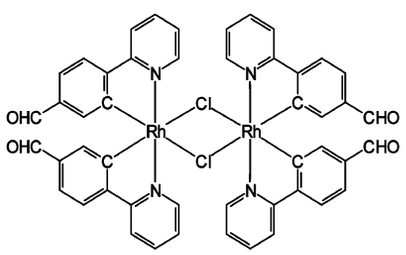

(**1**)

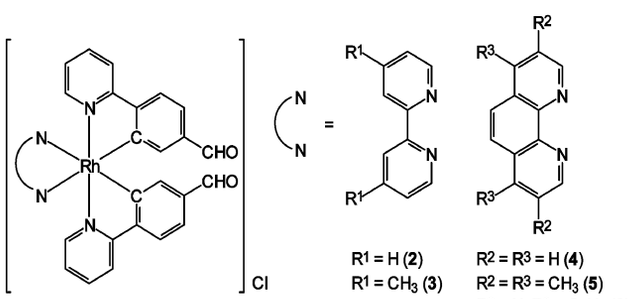

Scheme 1 Structures of complexes **1**–**6**.

Results and discussion

Synthesis

The dimeric precursor complex $[Rh_2(pba)_4Cl_2]$ (**1**) is obtained by refluxing a mixture of $RhCl_3 \cdot 3H_2O$ and Hpba in ethanol–water (3 : 1 v/v) for 24 h in the dark under an inert atmosphere

DOI: 10.1039/b310899f

of nitrogen. The monomeric complexes $[Rh(pba)_2(N–N)]Cl$ are prepared by refluxing complex **1** with 2 equivalents of the diimine ligand (N–N) in a mixture of methanol–dichloromethane (1 : 1 v/v) for 4 h in the dark under an inert atmosphere of nitrogen. The complexes are purified by recrystallisation to afford yellow crystals. All the complexes give satisfactory elemental analysis and are characterised by ^{1}H NMR, IR and positive ESI-MS. The aldehyde moieties of complexes **1**–**6** are characterised by a singlet at *ca.* δ 9.52–9.82 in the ^{1}H NMR spectra and an intense IR absorption band at *ca.* 1680 cm^{-1}. The X-ray crystal structures of complexes **1**, **3** and **4** are also studied.

X-Ray crystal structure determination

The perspective views of complex **1** and the complex cations of **3** and **4** are shown in Figs. 1, 2 and 3, respectively. The crystal determination data are listed in Table 1. Selected bond distances and angles of **1** are tabulated in Table 2 and those of complexes **3** and **4** in Table 3. For the dichloro-bridged dimer complex **1**, each rhodium(III) centre adopts a distorted octahedral geometry. The angles of the *trans* ligands at the metal centre are 172.6(3)° for N(1)–Rh(1)–N(2) and 173.9(2)° for N(3)–Rh(2)–N(4). The Rh–C bonds of the pba^- ligands show a mutual *cis* orientation around both rhodium(III) centres. Similar observations have been commonly found in other cyclometallated rhodium(III) [2b,3a,12,13] and iridium(III) [2a,b] systems. The

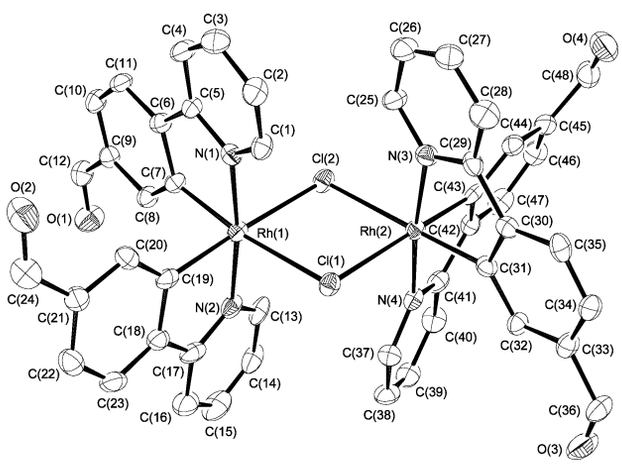

Fig. 1 Perspective view of complex **1** with the atomic numbering scheme. Hydrogen atoms are omitted for clarity. Thermal ellipsoids are shown at the 30% probability level.

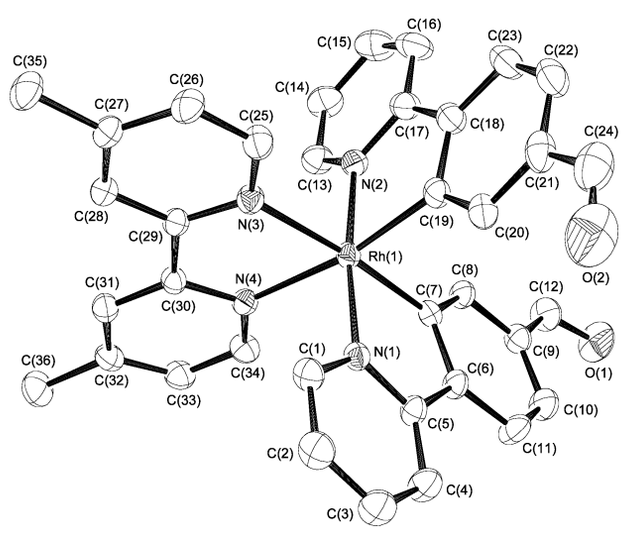

Fig. 2 Perspective view of complex cation of **3** with the atomic numbering scheme. Hydrogen atoms are omitted for clarity. Thermal ellipsoids are shown at the 30% probability level.

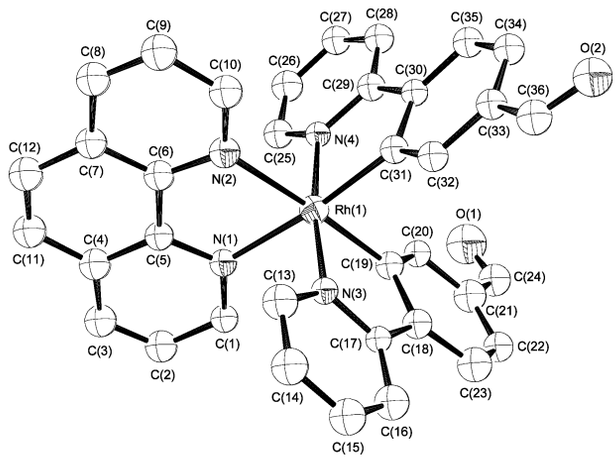

Fig. 3 Perspective view of complex cation of **4** with the atomic numbering scheme. Hydrogen atoms are omitted for clarity. Thermal ellipsoids are shown at the 30% probability level.

distances between the oxygen atoms of the two aldehyde groups attached to the same rhodium centre are *ca.* 8.6–8.8 Å. The bite angles of the pba^- ligands (*ca.* 81.1°) are very similar to that of the Cl–Rh–Cl angle (*ca.* 83.6°). These findings are also observed in other dichloro-bridged dirhodium(III) complexes with cyclometallating ligands. [3a,12]

The rhodium centres of both complexes **3** and **4** also adopt a distorted octahedral geometry. The angles of the *trans* ligands at the rhodium centre range between 170.05(18) and 176.3(4)°. Similar to complex **1**, a mutual *cis* orientation is also observed between the Rh–C bonds around the rhodium(III) centre. The Rh–N (diimine) bond lengths of complexes **3** (2.160(4) and 2.153(4) Å) and **4** (2.173(8) and 2.163(8) Å) are slightly longer than those of Rh–N (pba^-) (2.062(4) and 2.040(4) Å for **3**; 2.046(8) and 2.041(8) Å for **4**). This is a consequence of the *trans*-influence of the strong σ-donating carbon atoms of the pba^- ligands. Similar findings have also been reported in other related cyclometallated rhodium(III) [4b] and iridium(III) [14,15] polypyridine complexes. The N–Rh–N bite angles of the 4,4′-Me_2bpy (76.23(16)°) and phen (77.5(3)°) ligands in complexes **3** and **4**, respectively, are smaller than the average C–Rh–N bite angles of the pba^- ligands (80.7° for **3** and 81.3° for **4**). The separations between the oxygen atoms of the two aldehyde groups (*ca.* 9.3 and 9.5 Å for complexes **3** and **4**, respectively) are longer than those observed in complex **1**.

Electronic absorption and luminescence properties

The electronic absorption spectral data for complexes **1**–**6** are summarised in Table 4. The electronic absorption spectra of complexes **1** and **4** in dichloromethane at 298 K are shown in Fig. 4 as examples. The electronic absorption spectrum of **1** shows intense absorption bands and shoulders at *ca.* 249–321 nm, together with less intense low-energy absorption bands and shoulders at *ca.* 358–424 nm. The high-energy absorption bands are assigned to spin-allowed intra-ligand (^{1}IL) ($\pi \longrightarrow \pi^*$)($pba^-$) transitions. In view of the increased electron density on the rhodium centres due to the chloro ligands, the lower-energy absorption features are assigned to spin-allowed metal-to-ligand charge-transfer ^{1}MLCT (d_π(Rh) $\longrightarrow \pi^*(pba^-)$) transitions. Similar assignments have been reported in other related cyclometallated rhodium(III) systems. [2e,5a]

The electronic absorption spectra of complexes **2**–**6** show intense high-energy absorption bands and shoulders at *ca.* 223–324 nm ($\varepsilon \approx 10^4$ dm^3 mol^{-1} cm^{-1}) and low-energy absorption bands and shoulders at *ca.* 350–398 nm ($\varepsilon \approx 10^3$ dm^3 mol^{-1} cm^{-1}). In view of the similar absorption energy observed in the related cyclometallated rhodium(III) diimine systems, [2c,3b–d,4b,c,5] the high-energy absorption bands and shoulders are assigned to ^{1}IL ($\pi \longrightarrow \pi^*$)(diimine and pba^-) transitions, and the

Table 1 Crystal data and summary of data collection and refinement for complexes **1**, **3** and **4**

	1	**3**	**4**
Empirical formula	$C_{50}H_{38}Cl_4N_4O_5Rh_2$	$C_{38}H_{36}Cl_5N_4O_4Rh$	$C_{36}H_{28}ClN_4O_4Rh$
M_r	1122.46	892.87	718.98
Crystal size/mm	0.3 × 0.15 × 0.1	0.5 × 0.2 × 0.15	0.15 × 0.15 × 0.1
T/K	253	253	253
λ/Å	0.71073	0.71073	0.71073
Crystal system	Triclinic	Triclinic	Triclinic
Space group	$P\bar{1}$ (no. 2)	$P\bar{1}$ (no. 2)	$P\bar{1}$ (no. 2)
a/Å	10.769(2)	11.624(2)	9.838(2)
b/Å	12.909(3)	13.444(3)	10.038(2)
c/Å	18.272(4)	13.649(3)	16.961(3)
α/°	75.29(3)	83.27(3)	72.98(3)
β/°	88.42(3)	83.22(3)	86.01(3)
γ/°	70.97(3)	71.20(3)	86.16(3)
V/Å^3	2318.4(9)	1997.9(7)	1595.8(5)
Z	2	2	2
D_c/g cm^{-3}	1.608	1.484	1.496
μ(Mo-Kα)/mm^{-1}	0.995	0.806	0.665
F(000)	1128	908	732
$2\theta_{max}$/°	50.70	50.90	49.80
Index ranges, hkl	−12 to 12	−13 to 13	−9 to 9
	−14 to 13	−16 to 16	−10 to 10
	−21 to 21	−16 to 16	−19 to 17
Reflections collected	9859	12966	4625
Independent reflections	6014	6732	2662
No. of data for structural analysis	3812	5463	1760
GOF on F^2 [a]	0.940	1.062	0.937
R_{int} [b]	0.0376	0.0324	0.0497
R_1, wR_2 ($I > 2\sigma(I)$) [c]	0.0517, 0.1354	0.0608, 0.1879	0.0584, 0.1397
Largest diff. peak, hole/e Å^{-3}	1.320, −0.984	1.469, −0.916	0.494, −0.487

[a] $R_{int} = \Sigma|F_o^2 - F_o^2(\text{mean})|/\Sigma[F_o^2]$. [b] GOF = $\{\Sigma[w(F_o^2 - F_c^2)^2]/(n - p)\}^{1/2}$, where n is the number of reflections and p is the total number of parameters refined. The weighting scheme is $w = 1/[\sigma^2(F_o^2) + (aP)^2 + (bP)]$, where P is $[2F_c^2 + \max(F_o^2,0)]/3$, $a = 0.0827$, 0.1447 and 0.0558 for complexes **1**, **3** and **4**, respectively; $b = 0.0$. [c] $R_1 = \Sigma||F_o| - |F_c||/\Sigma|F_o|$, $wR_2 = \{\Sigma[w(F_o^2 - F_c^2)^2]/\Sigma[w(F_o^2)^2]\}^{1/2}$.

Table 2 Selected bond lengths (Å) and angles (°) for complex **1**

Rh(1)–N(1)	2.056(6)	Rh(2)–N(3)	2.068(6)
Rh(1)–N(2)	2.058(7)	Rh(2)–N(4)	2.071(6)
Rh(1)–C(7)	1.986(8)	Rh(2)–C(31)	1.990(8)
Rh(1)–C(19)	2.008(8)	Rh(2)–C(43)	1.998(8)
Rh(1)–Cl(1)	2.563(2)	Rh(2)–Cl(1)	2.570(2)
Rh(1)–Cl(2)	2.546(2)	Rh(2)–Cl(2)	2.544(2)
N(1)–Rh(1)–N(2)	172.6(3)	N(3)–Rh(2)–N(4)	173.9(2)
N(1)–Rh(1)–C(7)	81.1(3)	N(3)–Rh(2)–C(31)	81.9(3)
N(1)–Rh(1)–C(19)	92.7(3)	N(3)–Rh(2)–C(43)	93.2(3)
N(1)–Rh(1)–Cl(1)	94.10(19)	N(3)–Rh(2)–Cl(1)	92.81(18)
N(1)–Rh(1)–Cl(2)	91.39(17)	N(3)–Rh(2)–Cl(2)	93.4(2)
N(2)–Rh(1)–C(7)	94.8(3)	N(4)–Rh(2)–C(31)	95.1(3)
N(2)–Rh(1)–C(19)	81.1(3)	N(4)–Rh(2)–C(43)	81.5(3)
N(2)–Rh(1)–Cl(1)	90.51(18)	N(4)–Rh(2)–Cl(1)	92.66(18)
N(2)–Rh(1)–Cl(2)	94.9(2)	N(4)–Rh(2)–Cl(2)	89.80(18)
C(7)–Rh(1)–C(19)	89.8(3)	C(31)–Rh(2)–C(43)	90.9(3)
C(7)–Rh(1)–Cl(1)	172.7(2)	C(31)–Rh(2)–Cl(1)	93.2(2)
C(7)–Rh(1)–Cl(2)	90.9(2)	C(31)–Rh(2)–Cl(2)	174.2(2)
C(19)–Rh(1)–Cl(1)	95.9(2)	C(43)–Rh(2)–Cl(1)	173.1(2)
C(19)–Rh(1)–Cl(2)	175.9(2)	C(43)–Rh(2)–Cl(2)	92.8(2)
Cl(1)–Rh(1)–Cl(2)	83.63(7)	Cl(1)–Rh(2)–Cl(2)	83.56(7)
Rh(1)–Cl(1)–Rh(2)	95.86(7)	Rh(1)–Cl(2)–Rh(2)	96.94(7)

Table 3 Selected bond lengths (Å) and angles (°) for complexes **3** and **4**

Complex **3**

Rh(1)–N(1)	2.062(4)	Rh(1)–N(4)	2.153(4)
Rh(1)–N(2)	2.040(4)	Rh(1)–C(7)	1.992(5)
Rh(1)–N(3)	2.160(4)	Rh(1)–C(19)	1.995(6)
N(1)–Rh(1)–N(2)	172.99(15)	N(2)–Rh(1)–C(19)	80.7(2)
N(1)–Rh(1)–N(3)	94.76(17)	N(3)–Rh(1)–N(4)	76.23(16)
N(1)–Rh(1)–N(4)	90.21(16)	N(3)–Rh(1)–C(7)	174.65(18)
N(1)–Rh(1)–C(7)	80.72(18)	N(3)–Rh(1)–C(19)	95.12(19)
N(1)–Rh(1)–C(19)	95.5(2)	N(4)–Rh(1)–C(7)	100.81(18)
N(2)–Rh(1)–N(3)	91.44(17)	N(4)–Rh(1)–C(19)	170.05(18)
N(2)–Rh(1)–N(4)	94.45(17)	C(7)–Rh(1)–C(19)	88.2(2)
N(2)–Rh(1)–C(7)	93.25(19)		

Complex **4**

Rh(1)–N(1)	2.173(8)	Rh(1)–N(4)	2.046(8)
Rh(1)–N(2)	2.163(8)	Rh(1)–C(19)	2.023(10)
Rh(1)–N(3)	2.041(8)	Rh(1)–C(31)	2.002(10)
N(1)–Rh(1)–N(2)	77.5(3)	N(2)–Rh(1)–C(31)	97.6(4)
N(1)–Rh(1)–N(3)	89.7(3)	N(3)–Rh(1)–N(4)	172.3(3)
N(1)–Rh(1)–N(4)	95.7(3)	N(3)–Rh(1)–C(19)	81.9(4)
N(1)–Rh(1)–C(19)	98.8(4)	N(3)–Rh(1)–C(31)	94.5(4)
N(1)–Rh(1)–C(31)	174.0(4)	N(4)–Rh(1)–C(19)	91.8(4)
N(2)–Rh(1)–N(3)	97.5(3)	N(4)–Rh(1)–C(31)	80.6(4)
N(2)–Rh(1)–N(4)	89.0(3)	C(19)–Rh(1)–C(31)	86.1(4)
N(2)–Rh(1)–C(19)	176.3(4)		

lower-energy absorption bands and shoulders are tentatively assigned to spin-allowed ^{1}MLCT (d_π(Rh) ⟶ π*(diimine and pba$^-$)) transitions. It is interesting to note that the low-energy absorption bands and shoulders of complexes **2**–**6** at *ca.* 350–398 nm are blue-shifted with respect to their respective iridium(III) counterparts $[Ir(pba)_2(N–N)]^+$ (λ_{abs} = 363–451 nm).[10] This hypsochromic shift in absorption energy from iridium(III) to rhodium(III) is in agreement with the assignment of ^{1}MLCT transitions in view of the lower d_π orbital energy of the rhodium(III) centre.

The photoluminescence properties of complexes **1**–**6** have been studied. Similar to other dichloro-bridged dimeric rhodium(III) systems,[2e,5a] complex **1** does not show any noticeable emission in solution at room temperature. However, the complex exhibits intense and long-lived green emission in alcohol glass at 77 K (Table 5). The emission spectrum displays a structured band with a peak maximum at 510 nm, and progressional spacings of *ca.* 1330–1860 cm^{-1} are observed. With reference to previous photophysical studies of related cyclometallated systems $[Rh_2(N–C)_4Cl_2]$,[2e,5a] the 77 K glass emission of complex **1** is assigned to an excited state of ^{3}IL (π ⟶ π*)(pba$^-$) character, probably with mixing of some

Table 4 Electronic absorption spectral data for complexes **1**–**6** at 298 K

Complex	Medium	λ_{abs}/nm (ε/dm^3 mol^{-1} cm^{-1})
1	CH_2Cl_2	249 (60885), 266 sh (58910), 304 (61710), 321 sh (49850), 358 sh (8930), 398 sh (7490), 424 (9270)
2	CH_3CN	240 (32990), 260 sh (31950), 274 (30655), 297 (36105), 309 (33780), 322 sh (21735), 372 sh (5550), 396 (6660)
	CH_2Cl_2	243 (23930), 260 (23815), 275 (23260), 298 (27270), 309 (25950), 324 sh (16030), 373 sh (3460), 398 (4770)
3	CH_3CN	263 (22265), 275 (21225), 297 (24350), 307 sh (22700), 324 sh (13680), 375 sh (2990), 398 (4010)
	CH_2Cl_2	257 (31160), 273 (28400), 295 (33420), 306 (30880), 320 sh (19490), 375 sh (3300), 396 (5100)
4	CH_3CN	226 (54825), 272 (55365), 295 (38360), 312 sh (29090), 322 sh (25010), 350 (6110), 395 (6825)
	CH_2Cl_2	273 (46350), 294 (32700), 312 (24880), 323 sh (20700), 353 (4725), 397 (5880)
5	CH_3CN	243 (38465), 279 (48365), 295 sh (36680), 313 sh (27265), 322 sh (22555), 354 sh (5870), 398 (6715)
	CH_2Cl_2	242 (28460), 280 (36180), 296 sh (27920), 313 sh (20675), 323 sh (16720), 375 sh (3440), 398 (4440)
6	CH_3CN	223 sh (40330), 271 sh (34970), 288 (43190), 312 sh (28200), 322 sh (24775), 365 (5750), 396 (4490)
	CH_2Cl_2	275 sh (37500), 290 (42920), 313 sh (30050), 324 sh (26050), 367 (6130), 398 (4780)

Table 5 Photophysical data for complexes **1**–**6**

Complex	Medium (T/K)	λ_{em}/nm	τ_o/μs	Φ	k_r/s^{-1}	k_{nr}/s^{-1}
1	Glass[a] (77)	510, 554, 598, 673 sh	92.78			
2	CH_2Cl_2 (298)	506, 545, 586 sh	4.40	0.016	3.6×10^3	2.2×10^5
	CH_3CN (298)	506, 545, 586 sh	6.63	0.030	4.6×10^3	1.5×10^5
	Glass[b] (77)	498, 538, 585, 638 sh	206.46			
3	CH_2Cl_2 (298)	506, 545, 586 sh	4.24	0.015	3.5×10^3	2.3×10^5
	CH_3CN (298)	506, 545, 586 sh	6.28	0.021	3.3×10^3	1.6×10^5
	Glass[b] (77)	499, 540, 585, 636 sh	188.25			
4	CH_2Cl_2 (298)	506, 545, 586 sh	4.25	0.017	4.0×10^3	2.3×10^5
	CH_3CN (298)	506, 545, 586 sh	7.92	0.030	3.8×10^3	1.2×10^5
	Glass[b] (77)	498, 538, 578, 636 sh	199.50			
5	CH_2Cl_2 (298)	506, 545, 586 sh	4.55	0.024	5.3×10^3	2.1×10^5
	CH_3CN (298)	506, 545, 586 sh	7.67	0.032	4.1×10^3	1.3×10^5
	Glass[b] (77)	501, 542, 584, 636 sh	199.48			
6	CH_2Cl_2 (298)	506, 545, 586 sh	4.94	0.025	5.1×10^3	2.0×10^5
	CH_3CN (298)	506, 545, 586 sh	8.68	0.028	3.2×10^3	1.1×10^5
	glass[b] (77)	499, 540, 578, 638 sh	206.04			

[a] CH_2Cl_2–EtOH–MeOH (1 : 4 : 1 v/v/v). [b] EtOH–MeOH (4 : 1 v/v).

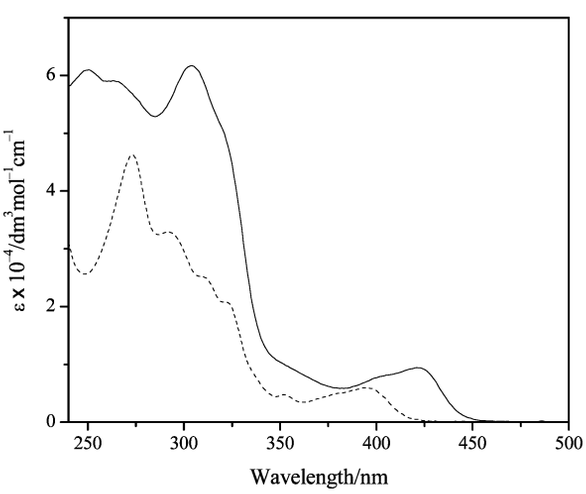

Fig. 4 Electronic absorption spectra of complexes **1** (—) and **4** (- - -) in CH_2Cl_2 at 298 K.

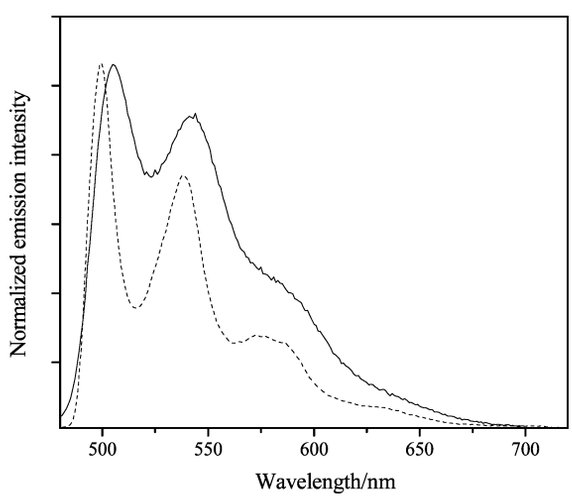

Fig. 5 Emission spectra of complex **2** in degassed CH_3CN at 298 K (—) and in EtOH–MeOH (4 : 1 v/v) at 77 K (- - -).

^{3}MLCT (d_π(Rh) ⟶ π*(pba$^-$)) character. The involvement of ^{3}MLCT character is supported by the observation that the emission maximum of **1** is *ca.* 1750 cm^{-1} higher in energy than that of its iridium(III) analogue $[Ir_2(pba)_4Cl_2]$ (λ_{em} = 560 nm), which is in line with the more stabilised d_π orbitals of rhodium(III) than those of iridium(III).

Upon photoexcitation, complexes **2**–**6** display long-lived and moderately intense greenish-yellow luminescence in solutions at 298 K and in low-temperature alcohol glass. The photophysical data are summarised in Table 5. The emission spectra of complex **2** in degassed CH_3CN at 298 K and in alcohol glass at 77 K are shown in Fig. 5. In solutions at 298 K, complexes **2**–**6** display similar and structured emission spectra with maxima at *ca.* 506 nm and progressional spacings of *ca.* 1280–1410 cm^{-1}. Remarkably, the luminescence lifetimes of complexes **2**–**6** in solutions at 298 K are extraordinarily long (*ca.* 4.2–8.7 μs). To the best of our knowledge, there is no precedent for such long emission lifetimes observed in other related cyclometallated rhodium(III) systems. For example, in degassed CH_3CN at room temperature, the emission lifetimes of the analogous complexes $[Rh(ppy)_2(bpy)]^+$ (Hppy = 2-phenylpyridine)[2c,3c,d,5b] and $[Rh(bzq)_2(phen)]^+$ (Hbzq = 7,8-benzoquinoline)[2c] are < 10 ns. Meanwhile, the complexes $[Rh(ppy)_2(N–N)]^+$ (N–N = 1,4,5,8-tetraazaphenanthrene, TAP; 1,4,5,8,9,12-hexaazatriphenylene, HAT) emit with a lifetime of 90–175 ns under similar conditions.[5b] Interestingly, the complex $[Rh(thpy)_2(bpy)]^+$ (Hthpy =

Table 6 Electrochemical data for complexes **1**–**6** at 298 K[a]

Complex	Oxidation $E_{1/2}$ or E_{pa}/V	Reduction $E_{1/2}$ or E_{pc}/V
1[b]	+1.47,[d] +1.70[e]	−1.60,[e] −1.74[e]
2[c]	+1.64[e]	−1.45,[d] −1.60,[e] −1.75,[e] −2.31,[e] −2.56[e]
3[c]	+1.68[e]	−1.50,[d] −1.65,[e] −1.78,[e] −2.30,[e] −2.54[e]
4[c]	+1.71[e]	−1.43,[d] −1.63,[e] −1.91,[e] −2.38,[e] −2.70[e]
5[c]	+1.64[e]	−1.52,[d] −1.67,[e] −1.87,[e] −2.38,[e] −2.73[e]
6[c]	+1.70[e]	−1.40,[d] −1.59,[e] −1.99,[e] −2.22,[e] −2.41[e]

[a] Glassy carbon electrode, sweep rate 0.1 V s^{-1}, all potentials *vs.* SCE. The hexafluorophosphate salts of **2**–**6** were used for electrochemical studies. [b] In CH_2Cl_2 (0.1 mol dm^{-3} TBAP). [c] In CH_3CN (0.1 mol dm^{-3} TBAP). [d] Quasi-reversible wave. [e] Irreversible wave.

2-(2-thienyl)pyridine) also displays a long emission lifetime (1 μs) under ambient conditions, and the excited state has been confirmed to be ^{3}IL(thpy$^-$) in character.[3d] In the current work, the observations of (i) the independence of the emission energy on the diimine ligands, (ii) the structured emission spectra and (iii) the long emission lifetimes all suggest that the emission originates from an excited state of predominant ^{3}IL ($\pi \longrightarrow \pi^*$)(pba$^-$) character. This assignment is in agreement with previous spectroscopic studies on other cyclometallated rhodium(III) complexes $[Rh(ppy)_2(N–N)]^+$ (N–N = bpy, phen)[2c,3b–d,4b–d,5b] and $[Rh(thpy)_2(bpy)]^+$.[3d] The emission properties of the current complexes are affected substantially by the aldehyde groups and it is probable that the electron-withdrawing properties of these substituents bring significant intraligand character to the excited-state of the complexes. In alcohol glass at 77 K, complexes **2**–**6** also display structured emission spectra with maxima at *ca.* 498–501 nm, and progressional spacings of *ca.* 1220–1630 cm^{-1}. In view of the very long emission lifetimes (188–206 μs) and the rich structural features of the emission bands, the emission is assigned to an excited state of ^{3}IL ($\pi \longrightarrow \pi^*$)(pba$^-$) character. Similar assignments have also been observed in related cyclometallated rhodium(III) systems.[2c,3b–d,4b–d,5] Besides, the excited states of the complexes in solutions at 298 K and in glass at 77 K probably possess some ^{3}MLCT (d_π(Rh) $\longrightarrow \pi^*$(pba$^-$)) character. The involvement of ^{3}MLCT character is supported by the observations that the 298 and 77 K emission maxima are *ca.* 966 and 850 cm^{-1} higher in energy than those of their iridium(III) counterparts $[Ir(pba)_2(N–N)]^+$ (λ_{em} = 532 and 520 nm at 298 and 77 K, respectively), which is in line with the fact that the d_π orbitals of rhodium(III) are more stabilised than those of iridium(III).

Electrochemical properties

The electrochemical properties of complexes **1**–**6** are studied by cyclic voltammetry. The electrochemical data are listed in Table 6. Complex **1** shows a quasi-reversible couple at +1.47 V *vs.* SCE in CH_2Cl_2 at 298 K, and an irreversible oxidation wave at +1.70 V. The quasi-reversible oxidation at +1.47 V is assigned to a metal-centred Rh^{IV}/Rh^{III} oxidation process. The occurrence of this couple at a higher potential than that of a related dimer $[Rh_2(ppy)_4Cl_2]$ (*ca.* +1.18 V *vs.* SCE)[2c,5b] is due to the electron-withdrawing ability of the pba$^-$ ligands, which renders the metal centres less electron-rich. On the other hand, the complex also shows irreversible waves at −1.60 and −1.74 V, which are attributed to the reduction of the cyclometallating pba$^-$ ligands in view of the fact that similar ligand-based reduction waves have also been observed for $[Ir_2(pba)_4Cl_2]$ (*ca.* −1.59 and −1.79 V).[10]

The cyclic voltammograms of complexes **2**–**6** in CH_3CN at 298 K show an irreversible wave at *ca.* +1.7 V. The potentials of the irreversible oxidation waves are higher than those of related $[Rh(ppy)_2(bpy)]^+$ (+1.58 V). This is in agreement with the assignment of metal-centred oxidations since the pba$^-$ ligand is more electron-withdrawing than the ppy$^-$ ligand, rendering the metal centre more difficult to be oxidised. In addition, complexes **2**–**6** also show a quasi-reversible reduction between −1.40 and −1.52 V and several irreversible waves between −1.6 and −2.7 V. With reference to the related systems $[Rh(ppy)_2(N–N)]^+$ (N–N = bpy, phen),[2c,3c,d,5b] the first reduction of complexes **2**–**6** is a diimine-centred process. This assignment is supported by the more negative potentials observed for both complexes **3** (−1.50 V) and **5** (−1.52 V), which is in line with the electron-donating ability of the methyl substituents on the 4,4′-Me_2bpy and 3,4,7,8-Me_4phen ligands.

Table 7 Photophysical data for bioconjugates **2-BSA**–**6-BSA** in Tris-Cl buffer (50 mM, pH 7.4) at 298 K

Conjugate	λ_{em}/nm	τ_o/μs (%)	Φ
2-BSA	526, 553, 609 sh	2.62 (44), 0.56 (56)	0.0073
3-BSA	525, 552, 608 sh	1.08 (38), 0.72 (62)	0.0055
4-BSA	523, 554, 608 sh	1.38 (41), 0.32 (59)	0.0060
5-BSA	522, 554, 608 sh	17.96 (43), 4.02 (57)	0.0053
6-BSA	523, 554, 608 sh	2.95 (40), 0.21 (60)	0.0059

Conjugation of BSA with complexes 2–6

Since the aldehyde group can react readily with primary amine group to form a secondary amine after reductive amination, complexes **2**–**6** can be considered as amine-specific biological labelling reagents. In this connection, we conjugate the protein BSA with complexes **2**–**6**. Although the separation of the bioconjugates of different stoichiometry is not attempted, any free labels present in the bioconjugates are removed by size-exclusion chromatography and membrane filtration. The electronic absorption spectra of the conjugates reveal intense absorption at 280 nm, attributable to both the protein and complex absorption, and other absorption features in the visible region mainly due to the rhodium(III) complexes. The dye-to-protein ratios (*D*/*P*) determined from the electronic absorption spectra of the free complexes and bioconjugates are *ca.* 0.4–0.9.

Upon photoexcitation, the bioconjugates **2-BSA**–**6-BSA** exhibit long-lived green emission in Tris-Cl buffer (50 mM, pH 7.4) at 298 K (Table 7). The emission spectra of these labelled proteins display structured bands with two maxima at *ca.* 523 and 554 nm, and a shoulder at *ca*. 608 nm. The emission of these rhodium(III)–BSA conjugates in aqueous buffer occurs at lower energy with respect to that of the free complexes in organic solvents. While this shift could be due to solvent effects, a change of excited-state nature is also a possible reason. Note that upon the bioconjugation, the electron-withdrawing aldehyde moieties of the complexes are converted to electron-donating secondary amines. Therefore, a rise in the π* energy level of the cyclometallating ligand is expected and an ^{3}IL state involving this ligand as the lowest-lying emissive state is not favoured. Instead, the emission is tentatively assigned to an ^{3}IL ($\pi \longrightarrow \pi^*$)(diimine) excited state, probably mixed with some ^{3}MLCT (d_π(Rh) $\longrightarrow \pi^*$(diimine)) character. The emission lifetimes of most of the conjugates are in the range of 0.2–3 μs, comparable to those of related biomolecules labelled with luminescent transition metal complexes.[10] However, the extra-

ordinarily long emission lifetime of **5-BSA** suggests that ^{3}IL ($\pi \longrightarrow \pi^*$)(3,4,7,8-$Me_4$phen) character is predominant in the excited state of this bioconjugate. Despite the low emission quantum yields of these conjugates, the emission lifetimes are sufficiently long to enable complexes **2**–**6** to be biological labels for time-resolved applications.

Conclusions

A series of cyclometallated rhodium(III) diimine complexes containing two aldehyde functional groups have been synthesised and characterised. The X-ray crystal structures of complexes **1**, **3** and **4** have been determined. The photophysical and electrochemical properties of these complexes have also been investigated. Structured emission bands with maxima at *ca.* 498–506 nm are observed for complexes **2**–**6** in both solutions at 298 K and alcohol glass at 77 K. The emission is tentatively assigned to an excited state of ^{3}IL ($\pi \longrightarrow \pi^*$)($pba^-$) character probably with some mixing of ^{3}MLCT (d_π(Rh) $\longrightarrow$ π^*(pba^-)) character. Interestingly, the luminescence lifetimes of the complexes in solutions at 298 K are much longer than those of other related cyclometallated rhodium(III) systems. Complexes **2**–**6** have been used to label BSA, and the bioconjugates have been isolated and purified. All the bioconjugates showed long-lived green luminescence upon photoexcitation. Labelling studies of other biomolecules with these luminescent rhodium(III) complexes are underway.

Experimental

General considerations

All syntheses were carried out under an atmosphere of nitrogen. Solvents were dried with appropriate reagents, distilled, degassed and stored under nitrogen.[16] The starting materials $RhCl_3 \cdot 3H_2O$, Hpba, bpy, 4,4′-Me_2bpy, phen, 3,4,7,8-Me_4phen and 4,7-Ph_2phen were purchased from Aldrich and used without further purification. $NaCNBH_3$ was obtained from Acros and used as received. Tetra-*n*-butylammonium hexafluorophosphate (TBAP) was from Aldrich and was recrystallised from hot ethanol and dried *in vacuo* at 110 °C before used. Unless stated otherwise, all the instruments for the characterisation, photophysical and electrochemical measurements were the same as described previously.[10] Luminescence quantum yields were measured using the optical dilute method[17] with an aerated aqueous solution of $[Ru(bpy)_3]Cl_2$ ($\Phi = 0.028$)[18] as the standard solution.

Synthesis

[Rh_2(pba)$_4Cl_2$] (1). A mixture of $RhCl_3 \cdot 3H_2O$ (157 mg, 0.60 mmol) and Hpba (436 mg, 2.38 mmol) in 20 ml ethanol–water (3 : 1 v/v) was refluxed for 24 h in the dark under an inert atmosphere of nitrogen. The pale yellow precipitate formed was collected by centrifugation and washed with 40 ml ethanol–water (95 : 5 v/v) and then air dried. The solid was then dissolved in dichloromethane (100 ml) and the solution was filtered with Celite. The filtrate was then evaporated to dryness to give a pale yellow solid. Subsequent recrystallisation from diffusion of diethyl ether into a dichloromethane–methanol (1 : 1 v/v) solution of the complex gave yellow crystals of **1**. Yield: 299 mg (50%). ^{1}H NMR (300 MHz, $CDCl_3$, 298 K, relative to TMS): δ 9.52 (s, 4H, CHO), 9.24 (d, J = 5.6 Hz, 4H, H5 of phenyl ring), 7.99–8.07 (m, 8H, H4 of pyridyl ring, H6 of phenyl ring), 7.74 (d, J = 7.9 Hz, 4H, H3 of pyridyl ring), 7.38 (d, J = 7.9 Hz, 4H, H6 of pyridyl ring), 6.98 (t, J = 7.3 Hz, 4H, H5 of pyridyl ring), 6.38 (s, 4H, H2 of phenyl ring). Anal. Calc. for $C_{48}H_{32}Cl_2N_4O_4Rh_2 \cdot 1/2CH_2Cl_2 \cdot CH_3OH$: C, 55.05; H, 3.45; N, 5.19. Found: C, 55.14; H, 3.58; N, 5.13%. IR (KBr) ν: 1680 cm^{-1} (CHO). Positive-ion ESI-MS (m/z): observed 466.9, calc. for $\{[Rh(pba)_2]\}^+$ 467.0.

[Rh(pba)$_2$(bpy)]Cl (2). A mixture of **1** (84 mg, 0.08 mmol) and bpy (25 mg, 0.16 mmol) in 20 ml methanol–dichloromethane (1 : 1 v/v) was refluxed for 4 h in the dark under an inert atmosphere of nitrogen. The yellow solution was then cooled to room temperature. A yellow solid was obtained after removal of the solvent. Subsequent recrystallisation from diffusion of diethyl ether into a dichloromethane solution of the complex gave yellow crystals of **2**. Yield: 90 mg (85%). ^{1}H NMR (300 MHz, acetone-d_6, 298 K, relative to TMS): δ 9.77 (s, 2H, CHO), 8.98 (d, J = 8.2 Hz, 2H, H6 and H6′ of bpy), 8.48 (d, J = 8.5 Hz, 2H, H5 of phenyl ring of pba^-), 8.36 (dt, J = 7.9 and 1.8 Hz, 2H, H4 and H4′ of bpy), 8.23–8.17 (m, 6H, H3 of pyridyl ring of pba^-, H3, H3′, H5 and H5′ of bpy), 7.95 (d, J = 5.9 Hz, 2H, H6 of pyridyl ring of pba^-), 7.73–7.66 (m, 4H, H4 of pyridyl ring of pba^-, H6 of phenyl ring of pba^-), 7.38 (t, J = 7.2 Hz, 2H, H5 of pyridyl ring of pba^-), 6.89 (s, 2H, H2 of phenyl ring of pba^-). Anal. Calc. for $C_{34}H_{24}ClN_4O_2Rh \cdot CH_2Cl_2 \cdot H_2O$: C, 55.17; H, 3.70; N, 7.35. Found: C, 54.99; H, 3.76; N, 7.17%. IR (KBr) ν: 1680 cm^{-1} (CHO). Positive-ion ESI-MS (m/z): observed 622.7, calc. for $\{[Rh(pba)_2(bpy)]\}^+$ 623.1.

[Rh(pba)$_2$(4,4′-Me$_2$bpy)]Cl (3). The synthetic procedure was similar to that of complex **2** except that 4,4′-Me_2bpy (30 mg, 0.16 mmol) was used instead of bpy. Subsequent recrystallisation from diffusion of diethyl ether into a dichloromethane solution of the complex gave yellow crystals of **3**. Yield: 89 mg (78%). ^{1}H NMR (300 MHz, acetone-d_6, 298 K, relative to TMS): δ 9.68 (s, 2H, CHO), 8.57 (d, J = 7.3 Hz, 2H, H5 of phenyl ring of pba^-), 8.34 (d, J = 7.9 Hz, 2H, H6 and H6′ of 4,4′-Me_2bpy), 8.12 (d, J = 8.2 Hz, 2H, H3 of pyridyl ring of pba^-), 8.06 (d, J = 8.2 Hz, 2H, H5 and H5′ of 4,4′-Me_2bpy), 7.85 (d, J = 5.3 Hz, 2H, H6 of pyridyl ring of pba^-), 7.73 (d, J = 5.6 Hz, 2H, H6 of phenyl ring of pba^-), 7.63 (m, 2H, H4 of pyridyl ring of pba^-), 7.39 (m, 2H, H3 and H3′ of 4,4′-Me_2bpy), 7.27 (dt, J = 6.2 and 1.2 Hz, 2H, H5 of pyridyl ring of pba^-), 6.80 (s, 2H, H2 of phenyl ring of pba^-), 2.56 (s, 6H, Me of 4,4′-Me_2bpy). Anal. Calc. for $C_{36}H_{28}ClN_4O_2Rh \cdot 1/2CH_2Cl_2 \cdot 2H_2O$: C, 57.27; H, 4.34; N, 7.32. Found: C, 57.42; H, 4.42; N, 7.09. IR (KBr) ν: 1680 cm^{-1} (CHO). Positive-ion ESI-MS (m/z): observed 650.8, calc. for $\{[Rh(pba)_2(4,4'\text{-}Me_2bpy)]\}^+$ 651.1.

[Rh(pba)$_2$(phen)]Cl (4). The synthetic procedure was similar to that of complex **2** except that phen (33 mg, 0.16 mmol) was used instead of bpy. Subsequent recrystallisation from diffusion of diethyl ether into a dichloromethane solution of the complex gave yellow crystals of **4**. Yield: 100 mg (87%). ^{1}H NMR (300 MHz, acetone-d_6, 298 K, relative to TMS): δ 9.80 (s, 2H, CHO), 8.99 (dd, J = 8.2 and 1.5 Hz, 2H, H2 and H9 of phen), 8.50 (d, J = 8.5 Hz, 2H, H5 of phenyl ring of pba^-), 8.49–8.45 (m, 4H, H3, H4, H7 and H8 of phen), 8.27 (d, J = 7.9 Hz, 2H, H3 of pyridyl ring of pba^-), 8.15–8.04 (m, 4H, H4 of pyridyl ring of pba^-, H5 and H6 of phen), 7.80 (d, J = 5.6 Hz, 2H, H6 of pyridyl ring of pba^-), 7.71 (d, J = 7.9 Hz, 2H, H6 of phenyl ring of pba^-), 7.23–7.19 (m, 2H, H5 of pyridyl ring of pba^-), 6.99 (s, 2H, H2 of phenyl ring of pba^-). Anal. Calc. for $C_{36}H_{24}ClN_4O_2Rh \cdot 1/2CH_2Cl_2 \cdot 2H_2O$: C, 57.57; H, 3.84; N, 7.36. Found: C, 57.78; H, 4.03; N, 7.57%. IR (KBr) ν: 1680 cm^{-1} (CHO). Positive-ion ESI-MS (m/z): observed 646.7, calc. for $\{[Rh(pba)_2(phen)]\}^+$ 647.1.

[Rh(pba)$_2$(3,4,7,8-Me$_4$phen)]Cl (5). The synthetic procedure was similar to that of complex **2** except that 3,4,7,8-Me_4phen (39 mg, 0.16 mmol) was used instead of bpy. Subsequent recrystallisation from diffusion of diethyl ether into a dichloromethane solution of the complex gave yellow crystals of **5**. Yield: 99 mg (80%). ^{1}H NMR (300 MHz, acetone-d_6, 298 K, relative to TMS): δ 9.79 (s, 2H, CHO), 8.54 (s, 2H, H2 and H9 of 3,4,7,8-Me_4phen), 8.50 (d, J = 7.9 Hz, 2H, H5 of phenyl ring of pba^-), 8.28 (d, J = 7.9 Hz, 2H, H3 of pyridyl ring of pba^-), 8.23 (s, 2H, H5 and H6 of 3,4,7,8-Me_4phen), 8.12 (dt,

J = 7.9 and 1.5 Hz, 2H, H4 of pyridyl ring of pba$^-$), 7.77 (d, J = 5.9 Hz, 2H, H6 of pyridyl ring of pba$^-$), 7.67 (dd, J = 7.9 and 1.5 Hz, 2H, H6 of phenyl ring of pba$^-$), 7.23–7.18 (m, 2H, H5 of pyridyl ring of pba$^-$), 6.96 (s, 2H, H2 of phenyl ring of pba$^-$), 2.86 (s, 6H, Me at C4 and C7 of 3,4,7,8-Me$_4$phen), 2.39 (s, 6H, Me at C3 and C8 of 3,4,7,8-Me$_4$phen). Anal. Calc. for $C_{40}H_{32}ClN_4O_2Rh\cdot 1/2CH_2Cl_2\cdot 2H_2O$: C, 59.49; H, 4.56; N, 6.85. Found: C, 59.75; H, 4.59; N, 6.88%. IR (KBr) v: 1680 cm^{-1} (CHO). Positive-ion ESI-MS (m/z): observed 702.8, calc. for {[Rh(pba)$_2$(3,4,7,8-Me$_4$phen)]}$^+$ 703.2.

[Rh(pba)$_2$(4,7-Ph$_2$phen)]Cl (6). The synthetic procedure was similar to that of complex **2** except that 4,7-Ph$_2$phen (55 mg, 0.16 mmol) was used instead of bpy. Subsequent recrystallisation from diffusion of diethyl ether into a dichloromethane–methanol (1 : 1 v/v) solution of the complex gave yellow crystals of **6**. Yield: 118 mg (85%). ^{1}H NMR (300 MHz, acetone-d$_6$, 298 K, relative to TMS): δ 9.82 (s, 2H, CHO), 8.60 (d, J = 4.9 Hz, 2H, H2 and H9 of 4,7-Ph$_2$phen), 8.56 (d, J = 8.2 Hz, 2H, H5 of phenyl ring of pba$^-$), 8.33 (d, J = 8.2 Hz, 2H, H3 of pyridyl ring of pba$^-$), 8.28 (s, 2H, H5 and H6 of 4,7-Ph$_2$phen), 8.17 (dt, J = 7.9 and 1.5 Hz, 2H, H4 of pyridyl ring of pba$^-$), 8.00 (d, J = 5.0 Hz, 2H, H3 and H8 of 4,7-Ph$_2$phen), 7.95 (d, J = 5.6 Hz, 2H, H6 of pyridyl ring of pba$^-$), 7.73–7.64 (m, 12H, H6 of phenyl ring of pba$^-$ and Ph of 4,7-Ph$_2$phen), 7.26–7.29 (m, 2H, H5 of pyridyl ring of pba$^-$), 7.01 (s, 2H, H2 of phenyl ring of pba$^-$). Anal. Calc. for $C_{48}H_{32}ClN_4O_2Rh\cdot CH_2Cl_2\cdot 1/2CH_3OH$: C, 63.51; H, 3.88; N, 5.98. Found: C, 63.53; H, 4.04; N, 6.11%. IR (KBr) v: 1680 cm^{-1} (CHO). Positive-ion ESI-MS (m/z): observed 799.1, calc. for {[Rh(pba)$_2$(4,7-Ph$_2$phen)]}$^+$ 799.2.

X-Ray structural analysis of complex 1. Single crystals of complex **1** were obtained from diffusion of diethyl ether into a dichloromethane–methanol (1 : 1 v/v) solution of the complex. A crystal of dimensions 0.3 × 0.15 × 0.1 mm mounted in a glass capillary was used for data collection at −20 °C on a MAR diffractometer with a 300 mm image plate detector using graphite-monochromatised Mo-Kα radiation (λ = 0.71073 Å). Data collection was made with 2° oscillation step of φ, 600 s exposure time and scanner distance at 120 mm; 100 images were collected. The images were interpreted and intensities integrated using the program DENZO.[19] The structure was solved by direct methods employing the SIR-97 program[20] on a PC. Rhodium, chlorine and many non-hydrogen atoms were located according to direct methods and successive least-squares Fourier cycles. Positions of other non-hydrogen atoms were found after successful refinement by full-matrix least-squares using the program SHELXL-97[21] on a PC. One dichloromethane and one methanol molecules were located, in which dichloromethane was disordered with chlorine atoms. Restrains were applied to assume similar C–Cl and Cl ··· Cl bond lengths or distances, respectively. One crystallographic asymmetric unit consists of one formula unit. In the final stage of least-squares refinement, non-hydrogen atoms of solvent molecules were refined isotropically, while other non-hydrogen atoms were refined anisotropically. Hydrogen atoms were generated by the program SHELXL-97. The positions of hydrogen atoms were calculated based on riding mode with thermal parameters equal to 1.2 times that of the associated carbon atoms, and participated in the calculation of final R indices. Due to the high displacement parameters of the non-hydrogen atoms of dichloromethane and methanol molecules, the hydrogen atoms of these solvent molecules were not generated, although they were included in the molecular formula.

X-Ray structural analysis of complex 3. Single crystals of complex **3** were obtained from the slow diffusion of diethyl ether vapour into a concentrated solution of the complex in dichloromethane. A crystal of dimensions 0.5 × 0.2 × 0.15 mm mounted in a glass capillary was used for data collection at −20 °C on a MAR diffractometer with a 300 mm image plate detector using graphite-monochromatised Mo-Kα radiation (λ = 0.71073 Å). Data collection was made with 2° oscillation step of φ, 600 s exposure time and scanner distance at 120 mm; 100 images were collected. The images were interpreted and intensities integrated using the program DENZO.[19] The structure was solved by direct methods employing the SIR-97 program[20] on a PC. Rhodium, chlorine and many non-hydrogen atoms were located according to direct methods and successive least-squares Fourier cycles. Positions of other non-hydrogen atoms were found after successful refinement by full-matrix least-squares using the program SHELXL-97[21] on a PC. The free chloride anion was located. Meanwhile, two water and two dichloromethane molecules were also located, in which one water and one dichloromethane were disordered. Restraints were applied to disordered molecules, assuming similar C–Cl, Cl ··· Cl bond lengths and distances, respectively. One crystallographic asymmetric unit consists of one formula unit, including one chloride anion, two water and two dichloromethane molecules. In the final stage of least-squares refinement, non-hydrogen atoms of disordered molecules were refined isotropically, while other non-hydrogen atoms were refined anisotropically. Hydrogen atoms were generated by the program SHELXL-97. The positions of hydrogen atoms were calculated based on riding mode with thermal parameters equal to 1.2 times that of the associated carbon atoms, and participated in the calculation of final R indices. Due to the high displacement parameters of the oxygen atoms of the two water molecules, the hydrogen atoms of these solvent molecules were not generated, although they were included in the molecular formula.

X-Ray structural analysis of complex 4. Single crystals of complex **4** were obtained from the slow diffusion of diethyl ether vapour into a concentrated solution of the complex in dichloromethane. A crystal of dimensions 0.15 × 0.15 × 0.1 mm mounted in a glass capillary was used for data collection at −20 °C on a MAR diffractometer with a 300 mm image plate detector using graphite-monochromatised Mo-Kα radiation (λ = 0.71073 Å). Data collection was made with 3° oscillation step of φ, 15 min exposure time and scanner distance at 120 mm; 60 images were collected. The images were interpreted and intensities integrated using the program DENZO.[19] The structure was solved by direct methods employing the SIR-97 program[20] on a PC. Rhodium and many non-hydrogen atoms were located according to direct methods and successive least-squares Fourier cycles. Positions of other non-hydrogen atoms were found after successful refinement by full-matrix least-squares using the program SHELXL-97[21] on a PC. One chloride anion and two water molecules were located randomly disorderedly in three positions and the occupancy for each chlorine was 1/3 and oxygen was 2/3. The ratio was also examined by free occupancy refinement. The oxygen atom of one aldehyde group was also disordered in the mode of flip. One crystallographic asymmetric unit consists of one formula unit. In the final stage of least-squares refinement, only rhodium was refined anisotropically, while the other atoms were refined isotropically. Hydrogen atoms were generated by the program SHELXL-97. The positions of hydrogen atoms were calculated based on riding mode with thermal parameters equal to 1.2 times that of the associated carbon atoms, and participated in the calculation of final R indices. Due to the high displacement parameters of the oxygen atoms of the two water molecules, the hydrogen atoms of these solvent molecules were not generated, although they were included in the molecular formula.

CCDC reference numbers 219240–219242.

See http://www.rsc.org/suppdata/dt/b3/b310899f/ for crystallographic data in CIF or other electronic format.

Conjugation of BSA with complexes 2–6

In a typical labelling reaction, the rhodium(III) complex (7.8 μmol) in 200 μl anhydrous DMSO was added to BSA (9.4 mg, 0.14 μmol) in 800 μl carbonate buffer (50 mM, pH 9.0). After the solution was stirred slowly in the dark at room temperature for 4 h, $NaCNBH_3$ (4.9 mg, 78 μmol) in 20 μl 2 M NaOH was added to the solution. The solution was stirred for 12 h in the dark at room temperature. The solution was then loaded onto a PD-10 column (Pharmacia) that had been equilibrated with Tris-Cl (50 mM, pH 7.4). The first band was collected. The solution was then concentrated with a YM-30 centricon (Amicon) and the conjugates were washed with Tris-Cl buffer successively to remove any free labels. Finally, the bioconjugates were purified by size-exclusion HPLC and stored at 4 °C before use.

Acknowledgements

We thank the City University of Hong Kong (Project No. 7100272) for financial support. K. K.-W. L. thanks the Faculty of Science and Engineering for financial support (Young/Junior Scholars Scheme). We are grateful to Professor Vivian W.-W. Yam of The University of Hong Kong for access to the equipment for photophysical measurements.

References

1 See, for example: (*a*) D. M. Roundhill and J. P. Fackler, Jr., *Optoelectronic Properties of Inorganic Compounds*, Plenum Press, New York, 1999; (*b*) D. M. Roundhill, *Photochemistry and Photophysics of Metal Complexes*, Plenum Press, New York, 1994; (*c*) K. Kalyanasundaram, *Photochemistry of Polypyridine and Porphyrin Complexes*, Academic Press, London, 1992; (*d*) V. Balzani and F. Scandola, *Supramolecular Photochemistry*, Ellis Horwood, London, 1991.

2 (*a*) F. O. Garces, K. Dedeian, N. L. Keder and R. J. Watts, *Cryst. Struct. Commun.*, 1993, **C49**, 1117; (*b*) F. O. Garces, K. A. King and R. J. Watts, *Inorg. Chem.*, 1988, **27**, 3464; (*c*) Y. Ohsawa, S. Sprouse, K. A. King, M. K. DeArmond, K. W. Hanck and R. J. Watts, *J. Phys. Chem.*, 1987, **91**, 1047; (*d*) M. Nishizawa, T. M. Suzuki, S. Sprouse, R. J. Watts and P. C. Ford, *Inorg. Chem.*, 1984, **23**, 1837; (*e*) S. Sprouse, K. A. King, P. J. Spellane and R. J. Watts, *J. Am. Chem. Soc.*, 1984, **106**, 6647.

3 (*a*) L. Ghizdavu, B. Kolp, A. von Zelewsky and H. Stoeckli-Evans, *Eur. J. Inorg. Chem.*, 1999, 1271; (*b*) A. Zilian, U. Maeder, A. von Zelewsky and H. U. Güdel, *J. Am. Chem. Soc.*, 1989, **111**, 3855; (*c*) D. Sandrini, M. Maestri, V. Balzani, U. Maeder and A. von Zelewsky, *Inorg. Chem.*, 1988, **27**, 2640; (*d*) M. Maestri, D. Sandrini, V. Balzani, U. Maeder and A. von Zelewsky, *Inorg. Chem.*, 1987, **26**, 1323.

4 (*a*) M. G. Colombo, A. Hauser and H. U. Güdel, *Inorg. Chem.*, 1993, **32**, 3088; (*b*) G. Frei, A. Zilian, A. Raselli, H. U. Güdel and H.-B. Büergi, *Inorg. Chem.*, 1992, **31**, 4766; (*c*) A. Zilian and H. U. Güdel, *Inorg. Chem.*, 1992, **31**, 830; (*d*) M. G. Colombo, A. Zilian and H. U. Güdel, *J. Am. Chem. Soc.*, 1990, **112**, 4581.

5 (*a*) L. Ghizdavu, O. Lentzen, S. Schumm, A. Brodkorb, C. Moucheron and A. Kirsch-De Mesmaeker, *Inorg. Chem.*, 2003, **42**, 1935; (*b*) P. Didier, I. Ortmans, A. Kirsch-De Mesmaeker and R. J. Watts, *Inorg. Chem.*, 1993, **32**, 5239.

6 R. P. Haugland, *Handbook of Fluorescent Probes and Research Chemicals*, Molecular Probes, Eugene, OR, 1996.

7 G. T. Hermanson, *Bioconjugate Techniques*, Academic Press, San Diego, CA, 1996.

8 (*a*) K. K. Sharma, H. Kaur and K. Kester, *Biochem. Biophys. Res. Commun.*, 1997, **239**, 217; (*b*) J. J. Kang, A. Tarcsafalvi, A. D. Carlos, E. Fujimoto, Z. Shahrokh, B. J. M. Thevenin, S. B. Shohet and N. Ikemoto, *Biochemistry*, 1992, **31**, 3288; (*c*) B. J. M. Thevenin, Z. Shahrokh, R. L. Williard, E. K. Fujimoto, J. J. Kang, N. Ikemoto and S. B. Shohet, *Eur. J. Biochem.*, 1992, **206**, 471.

9 (*a*) A. Sinz and K. Wang, *Biochemistry*, 2001, **40**, 7903; (*b*) H. Bhattacharjee and B. P. Rosen, *J. Biol. Chem.*, 1996, **271**, 24465; (*c*) J.-S. Kim and R. T. Raines, *Anal. Biochem.*, 1995, **225**, 174; (*d*) D. Mornet, K. Ue, P. Chaussepied and M. F. Morales, *Eur. J. Biochem.*, 1986, **159**, 555.

10 K. K.-W. Lo, C.-K. Chung and N. Zhu, *Chem. Eur. J.*, 2003, **9**, 475.

11 (*a*) J. L. Kisko and J. K. Barton, *Inorg. Chem.*, 2000, **39**, 4942; (*b*) B. A. Jackson and J. K. Barton, *Biochemistry*, 2000, **39**, 6176; (*c*) D. T. Odom, C. S. Parker and J. K. Barton, *Biochemistry*, 1999, **38**, 5155; (*d*) K. E. Erkkila, D. T. Odom and J. K. Barton, *Chem. Rev.*, 1999, **99**, 2777; (*e*) M. R. Arkin, E. D. A. Stemp, C. Turro, N. J. Turro and J. K. Barton, *J. Am. Chem. Soc.*, 1996, **118**, 2267; (*f*) D. Campisi, T. Morii and J. K. Barton, *Biochemistry*, 1994, **33**, 4130; (*g*) C. J. Murphy, M. R. Arkin, Y. Jenkins, N. D. Ghatlia, S. H. Bossmann, N. J. Turro and J. K. Barton, *Science*, 1993, **262**, 1025.

12 P. J. Steel, *J. Organomet. Chem.*, 1991, **408**, 395.

13 K. Polborn and K. Severin, *Eur. J. Inorg. Chem.*, 1998, 1187.

14 (*a*) F. Neve and A. Crispini, *Eur. J. Inorg. Chem.*, 2000, 1039; (*b*) F. Neve, A. Crispini, S. Campagna and S. Serroni, *Inorg. Chem.*, 1999, **38**, 2250; (*c*) V. Balzani, S. Campagna, G. Denti, A. Juris, S. Serroni and M. Venturi, *Coord. Chem. Rev.*, 1994, **132**, 1.

15 J. H. van Diemen, J. G. Haasnoot, R. Hage, E. Müller and J. Reedijk, *Inorg. Chim. Acta*, 1991, **181**, 245.

16 D. D. Perrin and W. L. F. Armarego, *Purification of Laboratory Chemicals*, Pergamon, Oxford, 1997.

17 J. N. Demas and G. A. Crosby, *J. Phys. Chem.*, 1971, **75**, 991.

18 K. Nakamaru, *Bull. Chem. Soc. Jpn.*, 1982, **55**, 2697.

19 Z. Otwinowski and W. Minor, *Methods Enzymol.*, 1997, **276**, 307.

20 A. Altomare, M. C. Burla, M. Camalli, G. L. Cascarano, C. Giacovazzo, A. Guagliardi, A. G. G. Moliterni, G. Polidori and R. Spagna, *J. Appl. Crystallogr.*, 1999, **32**, 115.

21 G. M. Sheldrick, Programs for Crystal Structure Analysis (Release 97–2), University of Göttingen, Germany, 1997.